Signatures of enhanced octupole correlations at high spin in ^{136}Nd

C. M. Petrache,[1] N. Minkov,[2] T. Nakatsukasa,[3,4,5] B. F. Lv,[1,6,7] A. Astier,[1] E. Dupont,[1] K. K. Zheng,[1] P. Greenlees,[8] H. Badran,[8] T. Calverley,[8,9] D. M. Cox,[8,*] T. Grahn,[8] J. Hilton,[8,9] R. Julin,[8] S. Juutinen,[8] J. Konki,[8,†] J. Pakarinen,[8] P. Papadakis,[8,‡] J. Partanen,[8] P. Rahkila,[8] P. Ruotsalainen,[8] M. Sandzelius,[8] J. Saren,[8] C. Scholey,[8] J. Sorri,[8,10] S. Stolze,[8,§] J. Uusitalo,[8] B. Cederwall,[11] A. Ertoprak,[11] H. Liu,[11] S. Guo,[6] M. L. Liu,[6] J. G. Wang,[6] X. H. Zhou,[6] I. Kuti,[12] J. Timár,[12] A. Tucholski,[13] J. Srebrny,[13] and C. Andreoiu[14]

[1]*Centre de Sciences Nucléaires et Sciences de la Matière, CNRS/IN2P3, Université Paris-Saclay, Bât. 104-108, F-91405 Orsay, France*
[2]*Institute of Nuclear Research and Nuclear Energy, Bulgarian Academy of Sciences, BG-1784 Sofia, Bulgaria*
[3]*Center for Computational Sciences, Univ. of Tsukuba, Tsukuba 305-8577, Japan*
[4]*Faculty of Pure and Applied Sciences, University of Tsukuba, Tsukuba, Ibaraki 305-8571, Japan*
[5]*RIKEN Nishina Center, Wako, Saitama 351-0198, Japan*
[6]*Institute of Modern Physics, Chinese Academy of Sciences, Lanzhou 730000, China*
[7]*School of Nuclear Science and Technology, Lanzhou University, Lanzhou 730000, China*
[8]*Department of Physics, University of Jyväskylä, Jyväskylä FIN-40014, Finland*
[9]*Department of Physics, University of Liverpool, The Oliver Lodge Laboratory, Liverpool L69 7ZE, United Kingdom*
[10]*Sodankylä Geophysical Observatory, University of Oulu, FIN-99600 Sodankylä, Finland*
[11]*KTH Department of Physics, S-10691 Stockholm, Sweden*
[12]*Institute for Nuclear Research, Hungarian Academy of Sciences, Pf. 51, H-4001 Debrecen, Hungary*
[13]*University of Warsaw, Heavy Ion Laboratory, Pasteura 5a, PL-02-093 Warsaw, Poland*
[14]*Department of Chemistry, Simon Fraser University, Burnaby, Canada BC V5A 1S6*

(Received 13 March 2020; revised 26 May 2020; accepted 2 July 2020; published 13 July 2020)

Experimental signatures of moderately enhanced octupole correlations at high spin in ^{136}Nd are indicated for the first time. The extracted dipole moments of two negative-parity bands are only two times smaller than those of the lanthanide nuclei with $N \approx 90$ which present well-established octupole correlations. Calculations using the cranked quasiparticle random phase approximation and a model of quadrupole-octupole rotations with octupole vibrations reveal the structure of the bands and the enhanced octupole correlations at high spin in ^{136}Nd.

DOI: 10.1103/PhysRevC.102.014311

I. INTRODUCTION

The medium- and high-spin states of the ^{136}Nd nucleus were the subject of many spectroscopic studies in the past [1–11], but also very recently new results were published from a high-statistics experiment performed with the JUROGAM II array at Jyväskylä, Finland [12–14] and from a lifetime experiment [15]. Investigations were also performed theoretically using different models, like the interacting boson model [16,17], the general Bohr Hamiltonian model [18], and more recently the triaxial projected shell model [19,20] and particle rotor model [21]. The relativistic Coulomb excitation measurement reported in Ref. [9] clearly showed that the ^{136}Nd nucleus is triaxial at low spin, with $\gamma \sim 25^\circ$. The different calculations also suggest a pronounced γ softness in nuclei with $N = 76$. Very recently, the existence of five chiral doublets was reported [12], which are based on four-quasiparticle configurations developing at medium spin. The observation of multiple chiral bands in ^{136}Nd is a clear indication that the triaxiality is sufficiently rigid at high spin to sustain the necessary three-dimensional (3D) chiral geometry. Another feature of the structure of ^{136}Nd is the existence of a negative-parity band that develops from low to very high spin, passing through a sequence of two crossings associated with large spin alignments. This band evolution was interpreted as the successive alignment of pairs of protons and neutrons, leading to stable triaxiality at high spin [5]. The configuration assigned to this negative-parity band is $\pi h^1_{11/2}(d_{5/2}, g_{7/2})^1$. Such a configuration would exhibit very small or no signature splitting between the odd- and even-spin levels of the band, because of the involvement of the high-Ω $\pi(d_{5/2}, g_{7/2})$ orbitals. However, this is not in agreement with the experimental data, which show a clear splitting between the odd- and even-spin members of the band, with the odd-spin levels shifted up. This was often speculated to be because of the presence of octupole correlations, which would mix with the odd-spin members of the negative-parity band and

*Present address: Department of Mathematical Physics, Lund Institute of Technology, S-22362 Lund, Sweden.
†Present address: CERN, CH-1211 Geneva 23, Switzerland.
‡Present address: Oliver Lodge Laboratory, University of Liverpool, Liverpool L69 7ZE, United Kingdom.
§Present address: Physics Division, Argonne National Laboratory, Argonne, Illinois 60439, USA.

would induce the lowering of the states. Such correlations are expected in nuclei with Fermi levels close to orbitals with $\Delta l = 3$, like $\pi(h_{11/2}, d_{5/2})$ and $\nu(f_{7/2}, i_{13/2})$ [22]. However, no clear experimental evidence of the existence of enhanced $E1$ and/or $E3$ transitions was reported until now in lanthanide nuclei with $N < 82$, where the contribution of the $\Delta l = 3$ neutron orbitals $\nu(f_{7/2}, i_{13/2})$ is negligible.

The present paper reports for the first time the existence of enhanced octupole correlations at high spins in ^{136}Nd, deduced from the observation of strong $E1$ transitions connecting the negative-parity bands to the positive-parity yrast band built on the two-quasiproton 10^+ state. The extracted electric dipole moments are large, slightly lower than those of the nuclei known to exhibit strong octupole correlations. Calculations employing the quasiparticle random phase approximation in the cranked shell model (cranked QRPA) and a model with quadrupole-octupole rotation and octupole vibration are used to investigate the existence of enhanced octupole correlations at high spin in ^{136}Nd.

II. EXPERIMENTAL RESULTS

High-spin states in ^{136}Nd were populated using the ^{100}Mo(^{40}Ar, 4n) reaction. The target consisted of a self-supporting enriched ^{100}Mo foil of 0.5 mg/cm^2 thickness and the 152-MeV beam of ^{40}Ar was provided by the K130 Cyclotron at the University of Jyväskylä, Finland. The ^{135}Nd and ^{136}Nd nuclei were the most strongly populated in the reaction, with cross sections of around 100 mb each. A total of 5.1×10^{10} threefold and higher prompt γ-ray coincidence events were accumulated using the JUROGAM II array. The events were time stamped by the total data readout (TDR) data acquisition, and sorted using the GRAIN code [23]. Fully symmetrized, three-dimensional (E_γ-E_γ-E_γ) and four-dimensional (E_γ-E_γ-E_γ-E_γ) matrices were analyzed using the RADWARE [24,25] analysis package. Spin and parity assignments were made on the basis of the measured DCO ratios ($R_{\rm DCO}$) of the transitions depopulating the states. Details of the data analysis are given in Ref. [13].

The partial level scheme of ^{136}Nd showing the bands $L5$ and $L6$ and their de-excitation to bands $L1$ and $N1$ is given in Fig. 1. The double-gated spectra showing the connecting transitions of the bands $L5$ and $L6$ to band $L1$ are given in Fig. 2. We identified a new $E1$ transition of 308 keV connecting the 9^- state of band $N1$ to the 8^+ state of the ground-state band (GSB), but more importantly, we identified three $E1$ transitions of 848, 950, and 1169 keV linking the bands $L5$ and $L6$ to band $L1$. These four $E1$ transitions were previously reported in Ref. [13]. $B(E1)/B(E2)$ ratios of the 7^- and 9^- states of band $N1$ and those of the 16^-, 17^-, and 19^- states of bands $L5$ and $L6$, and the resulting electric dipole moments are given in Table I and shown in Fig. 3. The electric dipole moments D_0 were obtained using the formula $D_0 = (5B(E1)/16B(E2))^{1/2} \times Q_0$, assuming a transition quadrupole moment $Q_0 = 2.7(2)\,eb$, equal to the value measured recently for the 12^+ state of band $L1$ [15]. We adopted the same Q_0 value for the transition quadrupole moments of bands $N1$, $L5$, and $L6$ based on the results of cranked Nilsson Strutinsky (CNS) calculations published in Ref. [13].

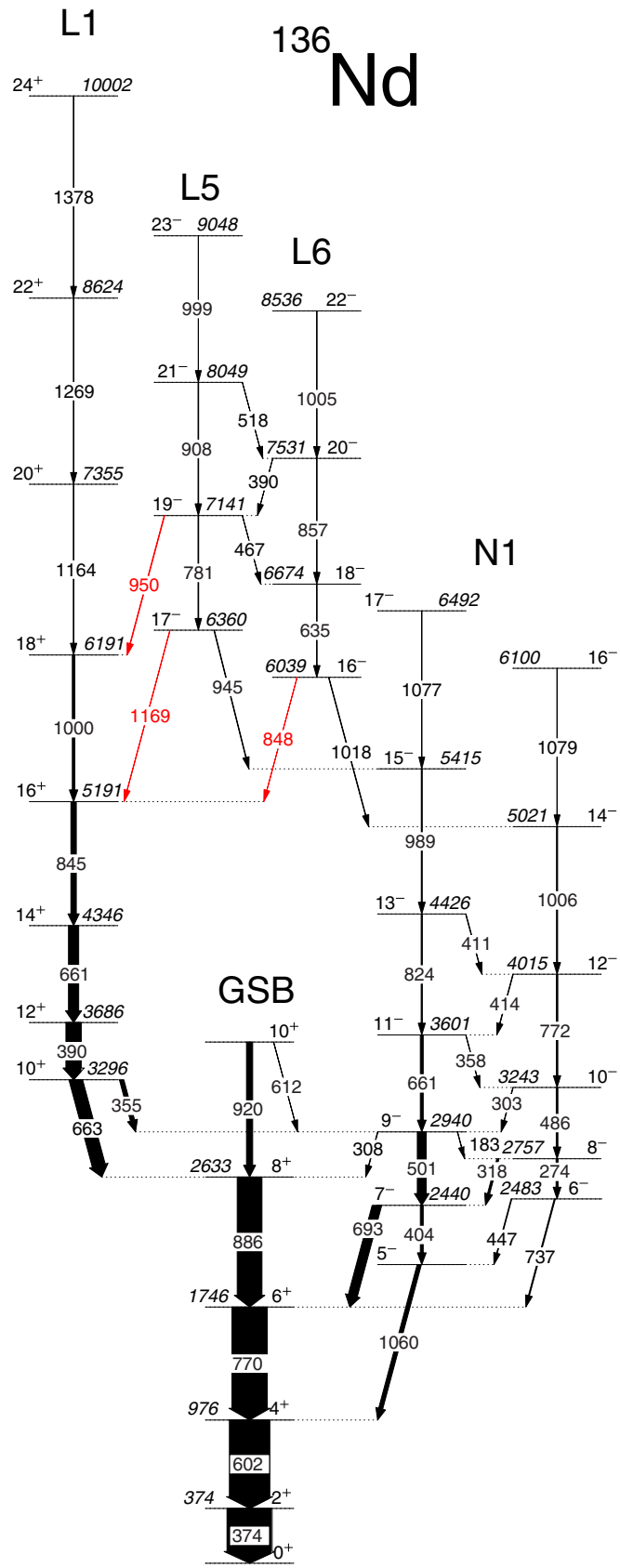

FIG. 1. Partial level scheme of ^{136}Nd showing the bands with enhanced octupole correlations $L5$ and $L6$, and their decay via $E1$ transitions (red color) to band $L1$.

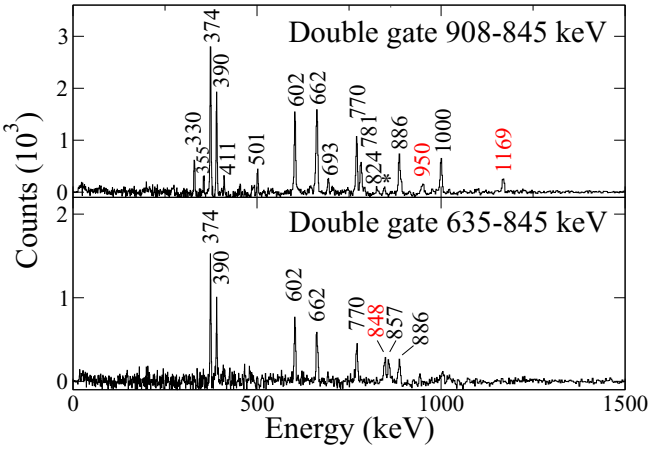

FIG. 2. Spectra constructed by double gating on the transitions above and below the connecting transitions between the bands with octupole correlations $L5$ and $L6$, and the band $L1$ of ^{136}Nd. The connecting transitions are marked with red labels, while the contaminant transitions are marked with an asterisk. In the upper spectrum the 330-keV transition connects band D6 reported in Ref. [13] to the 21^- state of band $L5$, while the 662-keV peak indicates the doublet composed of the 661-keV and 663-keV transitions of band $L1$.

In Table II of Ref. [13] is shown that the deformations (ε_2, γ) are $(\approx 0.18, \approx 25^\circ)$ for band $N1$ over the spin range 5^-–20^-, $(\approx 0.20, \approx 25^\circ)$ for band $L5$ over the spin range 17^-–23^-, and $(\approx 0.20, \approx 20^\circ)$ for band $L6$ over the spin range 16^-–20^-, which are all similar to those of band $L1$ of $(\approx 0.20, \approx 25^\circ)$ over the spin range 10^+–20^+, justifying thus the common adopted Q_0 for all discussed bands.

The electric dipole moments D_0 of the 16^- and 17^- levels of bands $L5$ and $L6$ can be overestimated, because are close to the crossing with band $N1$ where the $B(E2)$ value may be somewhat reduced because of band mixing. To take into account the systematic uncertainty introduced by the assumptions about the quadrupole strength we included an additional 20% uncertainty to the D_0 values.

One can see that the electric dipole moments of the high-spin states are a factor of 2 larger than those of the low-spin states, indicating enhanced octupole correlations, and a factor of 2 lower than those observed in the ^{146}Nd and ^{148}Nd nuclei situated in the region of strong octupole correlations [26,27].

TABLE I. Energies (E_γ) and intensities (I_γ) of connecting $E1$ transitions, $B(E1)/B(E2)$ values, and electric dipole moments D_0 of the bands in ^{136}Nd.

I	$\frac{E_\gamma(E1)}{E_\gamma(E2)}$	$\frac{I_\gamma(E1)}{I_\gamma(E2)}$	$\frac{B(E1)}{B(E2)}$ $(10^{-6}\mathrm{fm}^{-2})$	D_0 (e fm)
7^-	$\frac{693}{404}$	3.28(35)	0.082(12)	0.043(15)
9^-	$\frac{308}{501}$	0.055(15)	0.046(19)	0.029(21)
16^-	$\frac{848}{1018}$	0.28(5)	0.39(4)	0.094(30)
17^-	$\frac{1169}{945}$	0.46(6)	0.17(2)	0.062(20)
19^-	$\frac{950}{781}$	0.74(7)	0.19(4)	0.066(28)

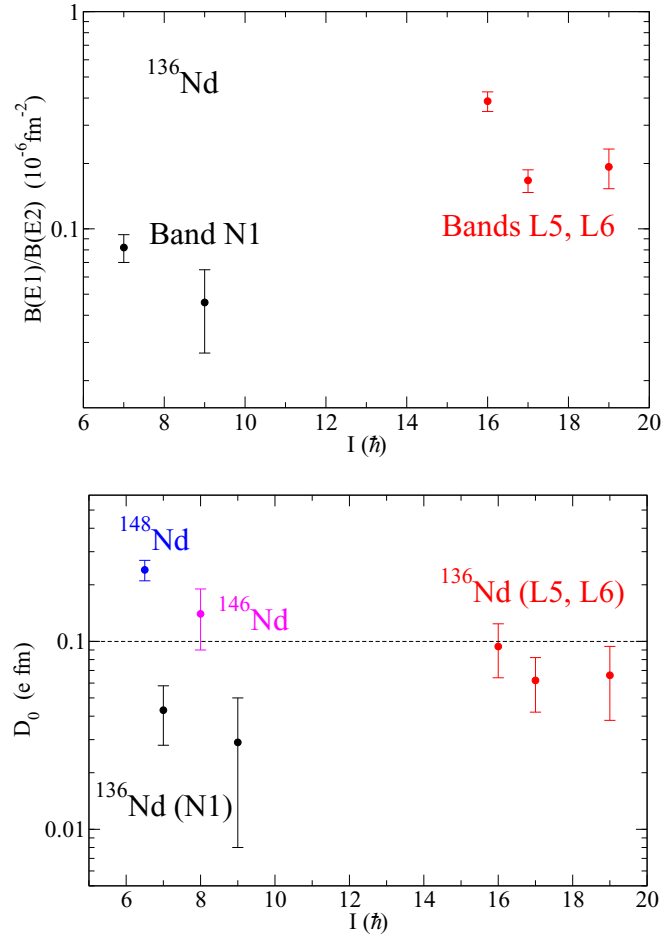

FIG. 3. Experimental $B(E1)/B(E2)$ ratios at low and high spin of ^{136}Nd. Experimental intrinsic $E1$ moments of low- and high-spin states of ^{136}Nd, compared with those of ^{146}Nd and ^{148}Nd.

The spin alignment i_x of bands $L5$, $L6$, $L1$ and the GSB of ^{136}Nd are shown in Fig. 4, as well as that of the continuation of bands $L5$ and $L6$ at low ($N1$) and high spin ($T3$ and $T4$, which are discussed in Ref. [13]). One can see that the spin alignment of band $N1$ at low spins is around $6\hbar$, being in agreement with the assigned $\pi h^1_{11/2}(d_{5/2}, g_{7/2})^1$ configuration [5]. A crossing occurs at a rotational frequency $\hbar\omega \sim 0.45$ MeV with a configuration involving two more protons in the $\pi h_{11/2}$ orbital, which increase the aligned spin by $\sim 8\hbar$, leading to a total aligned spin of $\sim 14\hbar$. A second crossing is observed at $\hbar\omega \sim 0.50$ MeV in both the odd- and even-spin sequences, leading to bands $T3$ and $T4$, which exhibit a gradual increase of the aligned spins after an initial jump of about $\sim 8\hbar$. This gradual increase of the aligned spin signals the alignment of a pair of neutrons in the intruder $\nu(f_{7/2}, h_{9/2})$ orbitals, which lead to a configuration with higher deformation and therefore higher moment of inertia. At the highest spin, band $T4$ exhibits a third crossing at a rotational frequency of about 0.62 MeV/$\hbar$, which must be because of the excitation of one neutron from a low-j $\nu(s_{1/2}, d_{3/2})$ orbital to the $\nu i_{13/2}$ intruder orbital. The configurations of bands $T3$ and $T4$ and the other high-spin bands of ^{136}Nd are discussed in detail in Ref. [13].

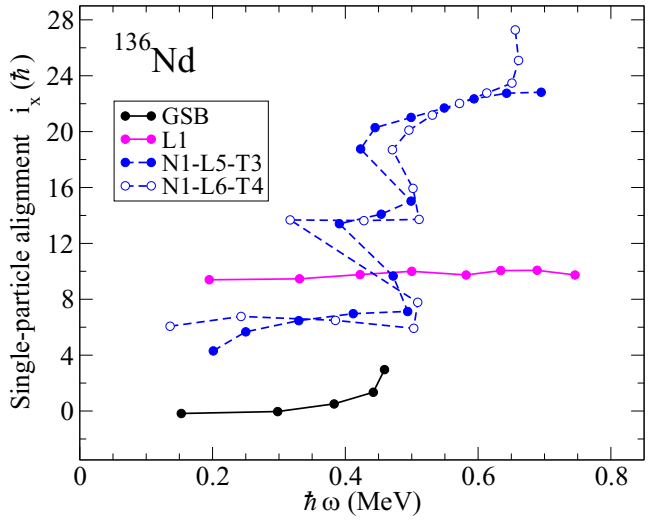

FIG. 4. Spin alignment i_x of the bands $L5$, $L6$, $L1$ and the GSB of ^{136}Nd. The spin alignments of the continuation of the bands $L5$ and $L6$ at low ($N1$) and high spin ($T3$ and $T4$, respectively) are also shown. The used Harris parameters are $J_0 = 10\,\hbar^2\text{MeV}^{-1}$ and $J_2 = 20\,\hbar^2\,\text{MeV}^{-3}$.

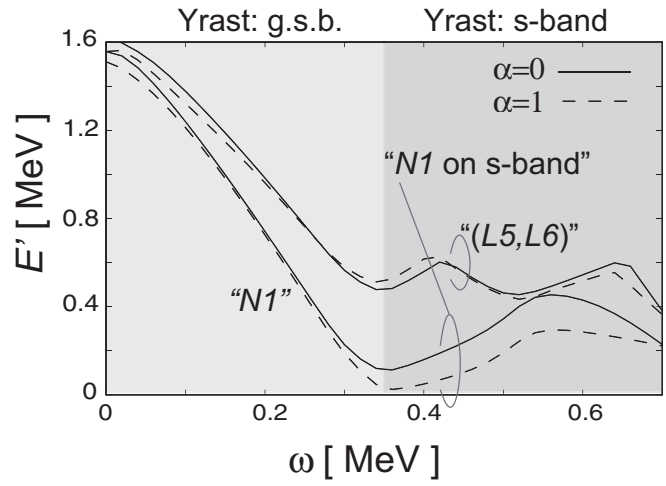

FIG. 5. Cranked QRPA calculations for ^{136}Nd showing the lowest and the next-lowest negative-parity states in each signature sector. Possible band assignment is indicated in the figure.

III. DISCUSSION

A. Cranked QRPA calculations

We performed calculations of the quasiparticle random phase approximation (QRPA) in the rotating frame [28–30]. The model is based on the cranked shell model, taking into account the residual interaction in the separable form of the isoscalar octupole type. At each rotational frequency ω, the yrast state is defined by the cranked Nilsson shell model with the monopole pairing interaction, on which the QRPA calculation was performed. The quadrupole deformation of the Nilsson potential is taken as $\delta_{\text{osc}} = 0.15$. See Ref. [30] for more details.

First of all, we must admit that the present calculations only provide a qualitative information. Because the shape of ^{136}Nd is transitional and its fluctuation is expected to be significant, the present treatment of the cranked QRPA based on the yrast band with a fixed deformation cannot give a quantitative answer. Nevertheless, we believe that it can provide a useful information on the octupole states at high spin.

Figure 5 shows the calculated Routhian plot of the lowest and the next-lowest negative-parity states in each signature sector. In the calculations, the crossing between the GSB and the s band takes place at $\hbar\omega \approx 0.35$ MeV, that is somewhat smaller than the observed crossing $\hbar\omega \approx 0.4$–0.45 MeV. The states at $\hbar\omega \approx 0$ can be regarded as the "octupole vibrations" based on the GSB. The lowest negative-parity state at $\hbar\omega = 0$ corresponds to the $K = 0$ octupole vibration with signature $\alpha = 1$ which has no signature partner. The second lowest state is $K = 0$ with both signature $\alpha = 0$ and 1. As the rotational frequency increases, they quickly lose their collectivity, becoming almost two-quasiparticle excitations. Consequently, the calculated intrinsic $E3$ transition amplitudes, which are a possible measure of the octupole collectivity, decrease by more than one order of magnitude between $\hbar\omega = 0$ and 0.3 MeV. This reduction of the collectivity is naturally expected, because the deformation of this nucleus is small. Many configurations of negative-parity two-quasiparticle states are quickly aligned and drastically lower their Routhian energy, becoming dominant at finite ω.

The calculated alignments of those negative-parity excitations are shown in Table II. The cranked QRPA calculations provide relative alignments $(i_x)_{\text{rel}}$ with respect to the yrast band on which the QRPA calculations are performed. Therefore, in the frequency range of $0.2 < \hbar\omega < 0.3$, when the excitation energy is built on the GSB, the values of $i_x = (i_x)_{\text{rel}}$ are shown in Table II. On the other hand, when the excitation is on the s-band, $(i_x)_s$, we add the alignment of the s band to the relative alignment $i_x = (i_x)_s + (i_x)_{\text{rel}}$. Assuming the observed band $L1$ is the s band, we adopt $(i_x)_s = 9\hbar$.

First of all, the alignment is beyond $3\hbar$ already at $\hbar\omega = 0.2$ MeV. Because the collective octupole vibration should carry the angular momentum $3\hbar$, this indicates a collapse of the collective phonon to an aligned two-quasiparticle state

TABLE II. Spin alignment of the first and second excited negative-parity QRPA excitations in ^{136}Nd. The alignment with respect to the yrast band $(i_x)_{\text{rel}}$ is obtained from the average slope of the calculated Routhians in a given range of ω. The alignment i_x is defined with respect to the GSB. See the text for details.

$\hbar\omega$ (MeV)	Signature	i_x ($\hbar$)	$(i_x)_{\text{rel}}$ ($\hbar$)	Possible candidates
0.2–0.3	$\alpha = 0$	5.1	5.1	$N1$
	$\alpha = 1$	5.4	5.4	$N1$
0.44–0.5	Lowest negative-parity state			
	$\alpha = 0$	6.9	−2.1	$N1$
	$\alpha = 1$	7.3	−1.7	$N1$
	Second-lowest negative-parity state			
	$\alpha = 0$	11.0	2.0	$L6$
	$\alpha = 1$	10.7	1.7	$L5$

[29]. In general, the alignment i_x relative to the GSB is always larger than $3\hbar$ in the observed range of the angular frequency $\hbar\omega > 0.15$ MeV. However, if we look at the alignment $(i_x)_{\rm rel}$ relative to the yrast band (s band), it is smaller than $3\hbar$ and sometimes negative. In the frequency range of $0.35 \leqslant \hbar\omega \leqslant 0.6$ MeV, the relative alignments for these four bands are calculated to be $|(i_x)_{\rm rel}| \lesssim 3\hbar$. Therefore, they could develop some octupole collectivity built on the s band ($L1$) at high spin.

In fact, the present cranked QRPA calculation suggests a moderate enhancement of octupole collectivity for bands $L5$ and $L6$ in the high-spin region. For instance, band $N1$ (the lowest negative-parity excited band) with $\alpha = 1$ calculated at $\hbar\omega = 0.3$ MeV carries the $E3$ transition amplitude of 15.4 $e$fm^3 to the GSB. The calculated alignment of band $N1$ relative to the GSB is about $5\hbar$. Therefore, it is natural to find the relatively small value of the $E3$ transition amplitude. This situation could be different if we switch the "vacuum" state of the QRPA excitation from the GSB to band s band ($L1$). In the present calculation, increasing $\hbar\omega$ further, the s band ($L1$) becomes the yrast band. At $\hbar\omega = 0.4$ MeV, the band $L5$ is calculated to carry the $E3$ amplitude of 34.6 $e$fm^3 to the band $L1$. This partial recovery of the octupole collectivity at high spins is made possible by its small relative alignment $|(i_x)_{\rm rel}| \lesssim 3\hbar$ that is within the range of the octupole-phonon excitation built on the band $L1$.

In experiment, the bands ($L5, L6$) are terminated around $\hbar\omega = 0.5$ MeV, then, switched to bands ($T3, T4$). In the calculations, candidates for ($T3, T4$) at $\hbar\omega = 0.5$ MeV are hardly identified because there are too many negative-parity excited states at high excitation energy. Nevertheless, the calculations provide some strongly aligned negative-parity two-quasiparticle states on the s band. At $\hbar\omega > 0.65$ MeV, the states with large alignments come down and we may see them in Fig. 5. This may be a possible indication of the bands ($T3, T4$) that have the alignment relative to the s band $(i_x)_{\rm rel} \approx 5\hbar$.

B. QORM calculations

To assess the eventual manifestation of octupole collectivity in ^{136}Nd we examine the possible formation of alternating-parity band (APB) structure in the level scheme of Fig. 1. It is known that APBs carry features inherent for the presence of pear-shape collective degrees of freedom in the nucleus [22]. The GSB and band $N1$ continue to higher spins through crossings with four-quasiparticle configurations involving two more protons in the $\pi h_{11/2}$ orbital. They cannot be combined into the same APB with the upper $L1$ and $L5$ bands. Thus, we have two sets of levels which could be eventually considered as two separate APBs: the first one including the GSB and band $N1$, and the second one including bands $L1$ and $L5$.

The levels which can be safely considered in the APB consisting of the GSB and band $N1$ are those with spins $I = 2^+, 4^+, 6^+, 8^+$ from the GSB and $I = 5^-, 7^-, 9^-, 11^-, 13^-, 15^-$ from band $N1$. The last levels with $I = 10^+$ from the GSB and $I = 17^-$ from band $N1$ are unsafe because of the presence of other close-lying states with the same angular momenta and energies in the neighboring bands. The minimal set of levels that can be taken into account in a fit procedure are those with $I = 2^+, 4^+, 6^+, 8^+$ of the GSB and with $I = 5^-, 7^-, 9^-$ of band $N1$, both sequences spanning almost the same energy interval below 3 MeV.

A detailed test of the APB structure is provided by a collective quadrupole-octupole (QO) model approach which with its two versions (limits), conditionally called "soft" and "rigid," is capable to distinguish between spectra corresponding to simultaneous axial quadrupole and octupole vibrations nonadiabatically coupled to rotation motion [31] and spectra in which relatively stable QO deformation is formed with the increasing of the angular momentum I [32]. In the former case the model potential corresponds to a soft QO shape providing a continuous (though decreasing with I) shift-up of the negative-parity levels with respect to the positive-parity levels. In the latter the system performs low-energy octupole oscillations sharply damped with the increase of I, so that the parity shift reaches zero value with possible reappearing with opposite sign (i.e., the positive-parity states appear shifted up with respect to the negative-parity ones) and essentially smaller magnitude. In this situation the APB acquires the structure of a single rotation band, the "octupole band." Because the octupole band corresponds to the rotation of a stable QO shape this version is called the QO rotation model (QORM) although it still involves octupole vibrations at low I. In QORM the octupole oscillations are considered within an angular-momentum-dependent double-well potential, while the most general dynamic behavior of the rotating QO shape involving contributions of various possible deformation modes is described through a point-symmetry-based rotation Hamiltonian [33].

Providing the above overall concept for the collective QO dynamics we notice that the APB structure consisting of the GSB and $N1$-band levels resembles the situation in the "rigid" limit represented by QORM. Despite the missing experimental 1^- and 3^- levels the available data suggest a sharply decreasing parity shift in low angular momenta with a sign inversion at moderate I, such that the structure changes from 5^- lying above 6^+, to 7^- lying well below 8^+. This behavior of the experimental spectrum obviously favors the interpretation provided by the QORM concept. We also remark that such a structure of the APB is typical for what is recognized as a stable QO mode observed in light actinides [32] and Ba and Ce nuclei (e.g., see [34]). Therefore, it can be expected that the application of the "rigid" QORM could provide a primary idea about the type of the eventual octupole collectivity observed. Still, in the present case the sharp parity-inversion effect at $I = 6^+, 7^-, 8^+$, if we consider the bands GSB and $N1$ of ^{136}Nd in terms of APB structure, appears to be a challenging problem. Therefore, the test results listed below provide a more qualitative rather than quantitative characteristic of the APB structure and give only a rough hint about the extent to which the spectrum may be associated with the presence of octupole collectivity.

Based on the above consideration, QORM model fits have been performed involving the levels with $I = 2^+, 4^+, 6^+, 8^+$ of the GSB and with $I = 5^-, 7^-, 9^-, 11^-, 13^-$ of band $N1$, obtaining a model description of these levels and predictions for the levels with $I = 1^-, 3^-$ and $I = 10^+, 12^+$ (details about

TABLE III. Experimental and QORM-calculated energies of the levels of the GSB (positive parity) and band $N1$ (negative parity) of ^{136}Nd.

I^π	E_{theory} (keV)	E_{exp} (keV)	E_{theory}–E_{exp} (keV)
1^-	1740	–	–
2^+	367	374	−7
3^-	1945	–	–
4^+	985	976	9
5^-	2057	2036	21
6^+	1776	1746	30
7^-	2408	2440	−32
8^+	2540	2633	−93
9^-	2978	2940	38
10^+	3276	–	–
11^-	3666	3601	65
12^+	4013	–	–
13^-	4396	4426	−30

the model and its application are given in Ref. [32]). We chose not to include the $I = 10^+$ level into the fit and instead to predict its energy, because of the above mentioned presence of two 10^+ experimental states with energies of 3296 keV ($L1$) and 3553 keV (GSB). The obtained QORM parameter values are $E_0 = 964$ keV, $B_3 = 28\ \hbar^2/\text{MeV}$, $\beta_{3\,\text{min}} = 0.13$, $d_1 = 0.04\ \text{MeV}^{-1}$, $d_2 = 0.5\ \text{MeV}^{-1}$, $A = 29$ keV, $A' = 1.3$ keV, $f_{11} = 1.7$ keV, and $f_{\text{qoc}} = -0.1$ keV. (See Ref. [32] for their explanation and physical meaning.)

The results of this test calculation are given in Table III. A good agreement between experiment and theory is obtained, even though the number of levels is limited and the number of parameters involved in the model is large. Nevertheless, the obtained result is still reasonable because all parameters, as, e.g., the octupole deformation $\beta_{3\,\text{min}}$, mass, and inertia parameters are somewhat constrained by their physical meaning [32]. In addition to that, part of the parameters, A', f_{11}, and f_{qoc}, obtained with small values, play a fine corrective role. The last two correspond to high-order QO interaction terms [32] which could be disregarded at first glance in the analysis of the overall APB structure. However, here we prefer to keep them in the calculation to make our analysis consistent with model applications in the well-recognized regions of octupole deformation. In the above description the rms deviation between theory and experiment is about 44 keV. In Fig. 6 we plotted the considered experimental and theoretical GSB and $N1$ band levels in the form of an APB. Here the $I = 1^-$, $I = 3^-$, $I = 10^-$, and $I = 12^-$ levels are predicted by the model. Also, we checked how the model description changes if the $I = 15^-$ level of band $N1$ is added to the fit procedure: The result essentially deteriorates to rms about 58 keV. Nevertheless, the above results open a way for possible interpretation of bands GSB and $N1$ in relation to octupole collectivity in ^{136}Nd. As seen from Fig. 6 the predicted overall structure of this part of the spectrum strongly resembles the low-energy structure of the nuclear octupole bands observed in light actinides [32] and Ba and Ce nuclei [34]. Also, it is interesting to remark that the theoretical prediction for the energy of the $I = 10^+$ level of 3275.5 keV is closer to the

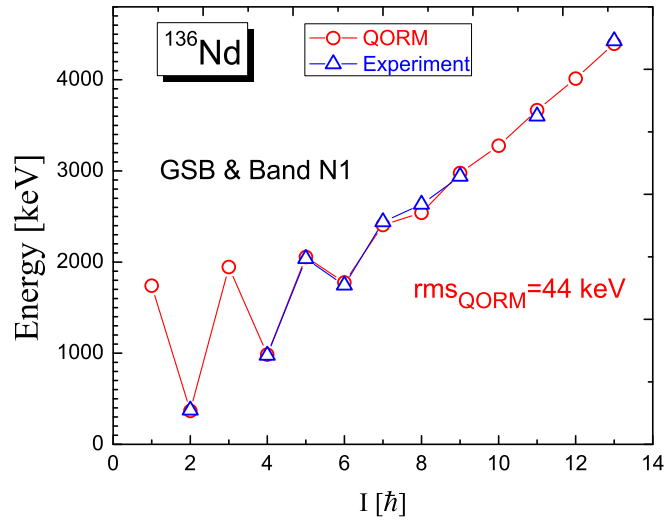

FIG. 6. QORM description of ^{136}Nd APB formed by GSB up to $I = 8^+$ and band $N1$ up to $I = 13^-$. See the text for the model parameters and explanation.

corresponding level of band $L1$ which has an energy of 3296 keV, rather than to the 3553-keV level of GSB.

It should be noted that the higher set of levels involving $L1$ and $L5$ can be interpreted as an APB in a similar way. To show this we made an independent QORM fit for this set of levels providing the parameter values $E_0 = 2209$ keV, $B_3 = 93\ \hbar^2/\text{MeV}$, $\beta_{3\,\text{min}} = 0.09$, $d_1 = 0.07\ \text{MeV}^{-1}$, $d_2 = 0.5\ \text{MeV}^{-1}$, $A = 12.5$ keV, $A' = 1.7$ keV, $f_{11} = 0.06$ keV, and $f_{\text{qoc}} = 0.03$ keV. The model description is illustrated in Fig. 7. Thus we see that an APB pattern similar to that in Fig. 6 can be obtained from $I = 10^+$ to $I = 23^-$ even though with a considerably larger rms=123 keV deviation between theory and experiment. One reason for the latter is that the starting levels of these two bands $I = 10^+$ and $I = 17^-$ appear in

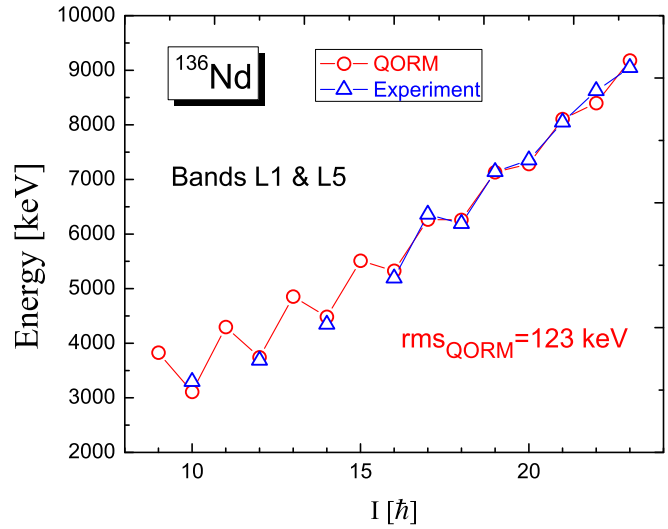

FIG. 7. QORM description of ^{136}Nd APB formed by band $L1$ from $I = 10^+$ to $I = 22^+$ and band $L5$ from $I = 17^-$ to $I = 23^-$. See the text for the model parameters and explanation.

somewhat different energy ranges which makes it hard for the model to keep the overall energy scale determined by the overall energy parameter $E_0 = 2209$ keV and the octupole mass parameter $B_3 = 93\,\hbar^2/\mathrm{MeV}$. Apart from that we observe a moderate change in the model parameters compared to the yrast APB. We recall again that the last three parameters, A', f_{11}, and f_{qoc}, play a corrective role with small values which practically do not affect the overall APB structure formed by the considered small amount of data. Additionally we remark that the parameter d_2 takes the same value of 0.5 MeV^{-1} in both calculated APBs while the shape of the double-well octupole-potential minima is adjusted through d_1 which slightly varies between the two sets of levels (see [32] for details on these parameters). Thus we see that although QORM is applied with a large number of parameters only part of them essentially determine the overall structure of the presently considered APB sets. However, we note that the eventual future appearance of additional new data, some of them predicted in Figs. 6 and 7, would certainly require the full contribution of all model parameters.

Further, we remark that the smaller value $A = 12.5$ keV of the inertia parameter indicates a much better rotation behavior of the set $L1\&L5$ compared to GSB&$N1$. In addition the octupole-parameter value $\beta_{3\,\mathrm{min}} = 0.09$ obtained in our fit of $L1$ and $L5$ appears lower than the yrast APB value of 0.13. Thus, the overall look at the two separate QORM fits of both APBs shows that if present the octupole collectivity in ^{136}Nd manifests with the octupole-deformation-potential minimum floating in the different energy ranges. This seems to be consistent with the lack of a definite nonzero octupole minimum in the microscopically obtained quadrupole-octupole PES.

Finally, we emphasize again that the overall structure of the two-level sets, $L1\&L5$ and GSB&$N1$ observed in Figs. 6 and 7 appears somewhat similar to that known for the APBs of nuclei with recognized octupole deformations [32,34]. Eventual future observation of lower-lying levels in band $L5$ may provide conditions for more consistent theoretical description of both APBs. Nevertheless, the so far obtained results point to the nucleus ^{136}Nd as a possible candidate for an interesting coexistence of γ-soft, triaxial, and quadrupole-octupole degrees of freedom.

IV. SUMMARY

Three transitions connecting high-spin negative- and positive-parity states of ^{136}Nd have been observed, from which a dipole moment two times larger than that at low spin and two times smaller than that of heavier Nd nuclei with strong octupole correlations is extracted. This represents an experimental evidence of moderately enhanced octupole correlations at high spin in a nucleus with $N < 82$, in which, at a difference from the nuclei with $N \approx 90$ presenting strong octupole correlations induced by both proton and neutron orbitals with $\Delta l = 3$, only the proton orbitals with $\Delta l = 3$ are active. Calculations using random phase approximation on two-quasiparticle configurations and a model with quadrupole-octupole rotations and vibrations qualitatively support the experimental results, showing an enhanced $E3$ strength between the negative-parity state and the s band. More extended calculations also including triaxiality would be more suitable for nuclei of this mass region, but this is beyond the scope of the present study, and can be the subject of future investigations. Systematic calculations and comparison with experiment in the chain of Nd and neighboring nuclei would also be welcome, to investigate the evolution of the negative-parity states and the possible octupole corrections not only as a function of proton and/or neutron number, but also as a function of spin.

ACKNOWLEDGMENTS

This work was supported by the Academy of Finland under the Finnish Centre of Excellence Programme (2012–2017), the EU 7th Framework Programme Project No. 262010 (ENSAR), the U.S. DOE under Contract No. DEFG02-95ER-40934, the National Research, Development and Innovation Fund of Hungary (Project No. K128947), the European Regional Development Fund (Contract No. GINOP-2.3.3-15-2016-00034), the National Research, Development and Innovation Office–NKFIH under Contract No. PD124717, the Polish National Science Centre under Grant No. 2013/10/M/ST2/00427, the Swedish Research Council under Grant No. 621-2014-5558, the Chinese Major State 973 Program No. 2013CB834400, the National Natural Science Foundation of China (Grants No. 11335002, No. 11375015, No. 11461141002, and No. 11621131001), the Natural Sciences and Engineering Research Council of Canada (NSERC), and the Bulgarian National Science Fund (BNSF) under Contract No. KP-06-N28/6. The use of germanium detectors from the GAMMAPOOL is acknowledged.

[1] E. S. Paul, C. W. Beausang, D. B. Fossan, R. Ma, W. F. Piel, Jr., P. K. Weng, and N. Xu, Phys. Rev. C **36**, 153 (1987).
[2] E. M. Beck, R. J. McDonald, A. O. Macchiavelli, J. C. Bacelar, A. Deleplanque, R. M. Diamond, J. E. Draper, and F. S. Stephens, Phys. Lett. B **195**, 531 (1987).
[3] R. M. Clark *et al.*, Phys. Lett. B **343**, 59 (1995).
[4] J. Billowes, K. P. Lieb, J. W. Noé, W. F. Piel, Jr., S. L. Rolston, G. D. Sprouse, O. C. Kistner, and F. Christancho, Phys. Rev. C **36**, 974 (1987).
[5] C. M. Petrache *et al.*, Phys. Lett. B **373**, 275 (1996).
[6] C. M. Petrache *et al.*, Phys. Rev. C **53**, R2581 (1996).
[7] C. M. Petrache, Z. Phys. A **358**, 225 (1997).
[8] S. Perries *et al.*, Phys. Rev. C **60**, 064313 (1999).
[9] T. Saito *et al.*, Phys. Lett. B **669**, 19 (2008).
[10] E. Mergel *et al.*, Eur. Phys. J. A **15**, 417 (2002).
[11] S. Mukhopadhyay *et al.*, Phys. Rev. C **78**, 034311 (2008).
[12] C. M. Petrache *et al.*, Phys. Rev. C **97**, 041304(R) (2018).
[13] B. F. Lv and C. M. Petrache *et al.*, Phys. Rev. C **98**, 044304 (2018).

[14] C. M. Petrache *et al.*, Phys. Rev. C **100**, 054319 (2019).
[15] A. Tucholski *et al.*, Phys. Rev. C **100**, 014330 (2019).
[16] G. L. Long, Phys. Rev. C **55**, 3163 (1997).
[17] D. Vretenar, S. Brant, G. Bonsignori, L. Corradini, and C. M. Petrache, Phys. Rev. C **57**, 675 (1998).
[18] L. Prochniak, K. Zaiac, K. Pomorski, S. G. Rohozinski, and J. Srebrny, Nucl. Phys. A **648**, 181 (1999).
[19] J. A. Sheikh, G. H. Bhat, R. Palit, Z. Naik, and Y. Sun, Nucl. Phys. A **824**, 58 (2009).
[20] S. Jehangir, G. H. Bhat, J. A. Sheikh, R. Palit, and P. A. Ganai, Nucl. Phys. A **968**, 48 (2017).
[21] Q. B. Chen, B. F. Lv, C. M. Petrache, and J. Meng, Phys. Lett. B **782**, 744 (2018).
[22] P. A. Butler and W. Nazarewicz, Rev. Mod. Phys. **68**, 349 (1996).
[23] P. Rahkila, Nucl. Instrum. Methods Phys. Res. A **595**, 637 (2008).
[24] D. Radford, Nucl. Instrum. Methods Phys. Res. A **361**, 297 (1995).
[25] D. Radford, Nucl. Instrum. Methods Phys. Res. A **361**, 306 (1995).
[26] W. Urban, R. M. Lieder, W. Gast, G. Hebbinghaus, A. Krämer-Flecken, T. Morek, T. Rzaca-Urban, W. Nazarewicz, and S. L. Tabor, Phys. Lett. B **200**, 424 (1988).
[27] W. Urban, R. M. Lieder, W. Gast, G. Hebbinghaus, A. Krämer-Flecken, T. Morek, T. Rzaca-Urban, W. Nazarewicz, and S. L. Tabor, Phys. Lett. B **258**, 293 (1991).
[28] T. Nakatsukasa, K. Matsuyanagi, S. Mizutori, and W. Nazarewicz, Phys. Lett. B **343**, 19 (1995).
[29] T. Nakatsukasa, Acta Phys. Pol. B **27**, 59 (1996).
[30] T. Nakatsukasa, K. Matsuyanagi, S. Mizutori, and Y. R. Shimizu, Phys. Rev. C **53**, 2213 (1996).
[31] N. Minkov, P. Yotov, S. Drenska, W. Scheid, D. Bonatsos, D. Lenis, and D. Petrellis, Phys. Rev. C **73**, 044315 (2006).
[32] N. Minkov, P. Yotov, S. Drenska, and W. Scheid, J. Phys. G **32**, 497 (2006).
[33] N. Minkov, S. B. Drenska, P. P. Raychev, R. P. Roussev, and D. Bonatsos, Phys. Rev. C **63**, 044305 (2001).
[34] N. Minkov, S. Drenska, and P. Yotov, in *Proceedings of the 35th International Workshop on Nuclear Theory (Rila, Bulgaria 2016),* Nuclear Theory, Vol. 35, edited by M. Gaidarov and N. Minkov (Heron Press, Sofia, 2016), p. 244.